INFN - Laboratori Nazionali di Frascati, May 1995
From: **The Second DaΦne Physics Handbook**[1]
Chapter 10: Two Photon Processes
Eds. L. Maiani, G. Pancheri, N. Paver

The Kinematics of the Two-photon Processes at DAΦNE

A. Courau
Laboratoire de l'Accélérateur Linéaire
CNRS-IN2P3-UNIVERSITE DE PARIS-SUD
91405 ORSAY FRANCE

1 Introduction

Let me recall that a $\gamma\gamma \to X$ process corresponds to a configuration of the reaction $ee \to eeX$ such that the cross section is dominated by the following double-peripheral graph:

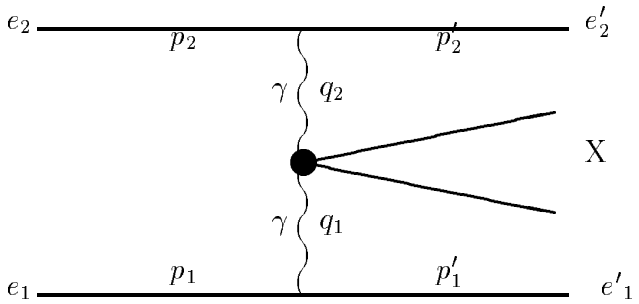

Figure 1: Two-photon process

This condition is generally satisfied for $\mid q^2_{1,2} \mid \ll M^2_X$.

If we compare the $\gamma\gamma$ production of hadrons at DAΦNE with respect to the hadronic production studied in other machines, we notice four main differences :

[1]Supported by the INFN, by the EC under the HCM contract number CHRX-CT920026 and by the authors home institutions

- The e^+e^- c.m. frame is not the Lab frame, since the beams cross at angle.

- The hadronic invariant mass W is small; On the other hand the ratio $W/2E_{beam}$, as well as the ratio of photon energy to beam energy E_γ/E_{beam}, are both larger than 0.1 (~ 0.3) instead of being generally lower ($\sim 10^{-2}$ to 10^{-1})

- The angular distibution of the scattered electrons is broader and less sharply peaked to very small angles

- The rapidity of the $\gamma\gamma$ system is limited by the phase-space and not by the central detector acceptance.

2 Notations

We use the following definitions where momenta, energies and angles are defined in the e^+e^- c.m. frame. (The same quantities when they are defined in the $\gamma\gamma$ frame will be indicated by a star superscript) .

p_i and E are respectively the four-momentum and the energy of the incident electrons.

p'_i , E'_i , Θ'_i and Φ'_i are respectively the four-momentum , the energy, the polar and azimuthal angle of either scattered electrons ($i = 1, 2$),

q_i , $E_{\gamma i}$, θ_i and ϕ_i are the same quantities for either virtual photon associated with a scattered electron ($i = 1, 2$),

k_j , E_j , Θ_j and Φ_j are the same quantities for the outgoing particles of the hadronic system produced,

W , $E_{\gamma\gamma}$, β are respectively the invariant mass, the energy and the absolute value of the velocity of the $\gamma\gamma$ system in the ee frame,

Δ is the acolinearity angle between the two scattered electrons ($\Delta = 0$ when the two electrons are back to back in the ee frame).

In addition we define dimensionless quantities :

$$X_i = E_{\gamma i}/E \quad ; \quad Z = W/2E \quad ; \quad Q^2 = -q^2/E^2$$

with $0 \leq X, Z \leq 1$

Let us note that m_π and m_e being respectively the pion mass and the electron mass, one has at DAΦNE $m_e/E \simeq 10^{-3}$, while $W \geq 2m_\pi$ involves $Z \geq 0.3$

3 Kinematic relations

Since, in practice, Θ'_i should be relatively small ($\Theta'_i \leq 0.3$) one has :

$$\hat{\Theta} \equiv 2\sin\Theta'/2 \simeq \Theta' \quad \text{and,} \quad \hat{\Delta} \equiv 2\sin\Delta/2 \simeq \Delta$$

Neglecting the electron mass (for $E, E' \gg m_e$), we obtain from $W^2 = (p_1 + p_2 - p'_1 - p'_2)^2$,
$E_{\gamma\gamma} = 2E - E'_1 - E'_2$ with , $E'_i = (1 - X_i)E$ the relations :

$$Z^2 = X_1 X_2 - \frac{1}{4}(1-X_1)(1-X_2)\hat{\Delta}^2$$
$$\beta^2 = \frac{(X_1 - X_2)^2 + (1-X_1)(1-X_2)\hat{\Delta}^2}{(X_1+X_2)^2}$$

Now from $q_i^2 = (p_i - p_i')^2$ one gets,

for $\Theta_i' = 0$ $\qquad -q_{i,min}^2 \cong -\tilde{q}_{i,min}^2 = \frac{X_i^2}{1-X_i} m_e^2$

for $\Theta_i' \gg m_e/E'$ $\qquad -q_i^2 \cong -\tilde{q}_i^2 = (1-X_i)E^2\hat{\Theta}^2$

and we write for the whole Θ_i range (dropping the i index): $q^2 = \tilde{q}_{min}^2 + \tilde{q}^2$

$$Q^2 \equiv -q^2/E^2 = \frac{X^2}{1-X}\left[(\frac{m_e}{E})^2 + (\frac{1-X}{X}\hat{\Theta})^2\right]$$
$$\hat{\Theta}^2 = \frac{1}{1-X}\frac{\mid q^2 \mid}{E^2} - (\frac{X}{1-X}\frac{m_e}{E})^2$$

and : $\qquad p_\perp'^2 \equiv \mid \overrightarrow{p'} \mid^2 \sin^2\Theta' \cong (1-X) \mid q^2 \mid$

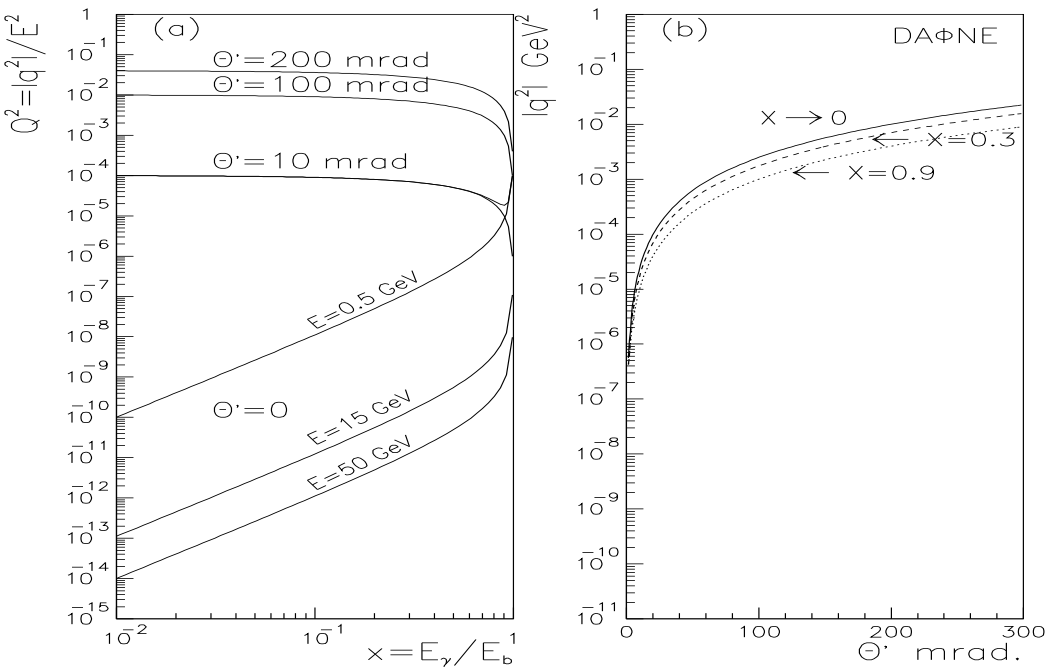

Figure 2: Relations between X , $\mid q^2 \mid$ and, Θ'

Let me make the following comments :

In Fig.2-a, X and Q^2 are plotted in logarithmic scales . Since the equivalent photon spectrum is proportional to $(dX/X)(dQ^2/Q^2)$ any area on this plot is proportional to the intensity of the photons flux. Then one notices that varying E or X practically changes the flux only at small angle. It results that the angular distribution of the scattered electrons becomes flatter when X is increased or E is decreased; it thus appears quite different for $X < 0.1$, $E > 10GeV$ and $X > 0.1$, $E < 1GeV$.

In Fig.2-b, the values of q^2 at DAΦNE ($E = 0.51 GeV$) are plotted in GeV^2. For $W = 300 MeV$, $W^2 \simeq 10^{-1} GeV^2$. Then $\mid q^2 \mid /W^2$ is just one order of magnitude larger than the q^2 values plotted on the figure. So, one notices that for $W \geq 300 MeV$, $\mid q^2 \mid /W^2$ remains small up to Θ' values of a few hundreds of milliradians

4 Quasi-real photons

In the $\gamma\gamma$ processes, because of the occurrence of the propagators $1/q_i^2$, small q_i^2 values play a dominent role : Those small q_i^2 values are obtained, whatever E_γ may be, when the corresponding electrons are scattered at very small angles.

If that is the case of both electrons, the cross section to be computed may be easily factorized, i.e. equivalent-photon spectra may be used for both virtual photons, which are then called "quasi-real". On the other hand, the Lorentz boost direction of the $\gamma\gamma$ system in the ee frame, as well as the $\gamma\gamma$ axis in the $\gamma\gamma$ frame, remain close to the ee axis in the ee c.m. frame [2], and one can derive the following simplified kinematic relations :

$$\begin{aligned} \Theta'_i \sim 0 \quad ; \quad \Phi'_i \simeq \Phi'^{\star}_i \\ Z^2 \simeq X_1 X_2 \quad ; \quad \beta \simeq \mid \frac{X_1 - X_2}{X_1 + X_2} \mid \\ \widetilde{\beta_j} \cos\Theta_j \simeq \frac{\beta - \widetilde{\beta}^{\star}_j \cos\Theta^{\star}_j}{1 - \beta \widetilde{\beta}^{\star}_j \cos\Theta^{\star}_j} \quad ; \quad \Phi_j \simeq \Phi^{\star}_j \end{aligned}$$

where $\widetilde{\beta}_j$, $\cos\Theta_j$ and $\widetilde{\beta}^{\star}_j$, $\cos\Theta^{\star}_j$ are respectively the velocity and the cosine along the ee axis of the outgoing particles in the ee and $\gamma\gamma$ c.m frames.

Using the rapidities instead of velocities

$$\begin{aligned} Y &\equiv \tanh^{-1}\beta \\ y_j &\equiv \tanh^{-1}(\widetilde{\beta}_j \cos\Theta_j) \\ y^{\star}_j &\equiv \tanh^{-1}(\widetilde{\beta}^{\star}_j \cos\Theta^{\star}_j) \end{aligned}$$

one has :

$$\begin{aligned} \Theta'_i \sim 0 \quad ; \quad \Phi'_i \simeq \Phi'^{\star}_i \\ Z^2 = X_1 X_2 \quad ; \quad Y = \frac{1}{2} \ln \frac{X_1}{X_2} \\ y_j = Y + y^{\star}_j \quad ; \quad \Phi_j = \Phi^{\star}_j \end{aligned}$$

Actually the quasi-reality condition which allows us to neglect all longitudinal terms and then to factorize the cross section is given by

$$\frac{\mid q^2_{1,2} \mid}{W^2} \ll 1$$

[2] more precisely, the transverse component of the Lorentz boost remains negligible

It is the the same conditions which also justify the kinematical approximations as described just above. We have shown in the previous section that, at DAΦNE, those conditions are satisfied for $W > 2m_\pi$ up to a few hundreds of milliradians (see fig.2). Let us notice that in this case $Z > 0.3$ while $X > Z^2 \simeq 0.1$ involves $X > 0.1$.

4.1 Hadronic-state production

Then, one has simple relations between equivalent sets of independent variables relative either to the photon energies X_1, X_2 or to the $\gamma\gamma$ system Z,β or Z,Y.

$$Z^2 = X_1 X_2 \quad , \quad Y = \frac{1}{2} \ln \frac{X_1}{X_2} \qquad \text{or} \quad X_{1,2} = Z e^{\pm Y}$$

while $X_1, X_2 \leq 1$ leads to :

$$Z^2 \leq X \leq 1 \qquad ; \qquad \ln(Z) \leq Y \leq \ln(1/Z)$$

Those relations are visualized, according to $\ln Z = \frac{1}{2}(\ln X_1 + \ln X_2)$ and, $Y = \frac{1}{2}(\ln X_1 - \ln X_2)$, on the Fig.3 where X_1 and X_2 are plotted on logarithmic scales.

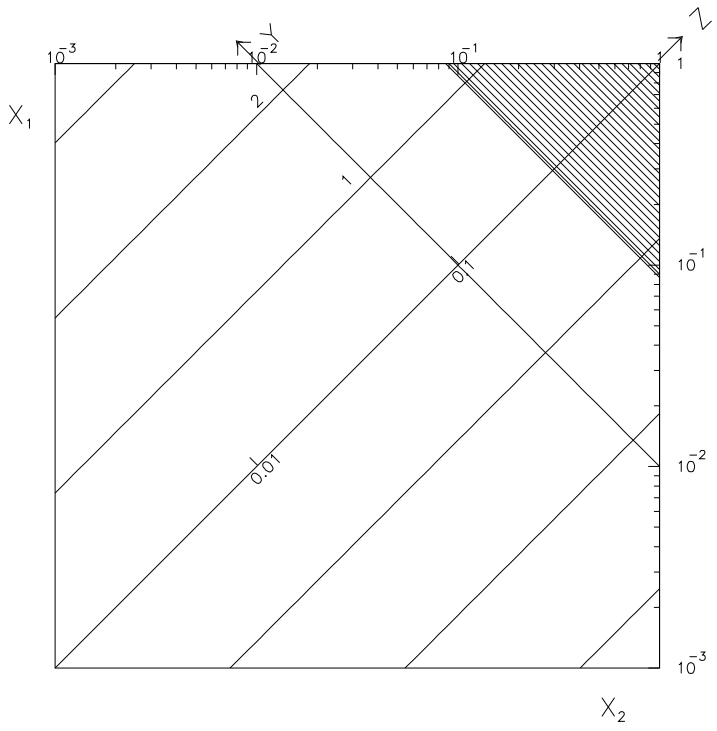

Figure 3: relations between X_1, X_2 and Z,Y

Let us make the following remarks :

- Since both photon spectra are proportional to dX/X, any area on this plot is also proportional to the $\gamma\gamma$ luminosity.

- The hatched area is the only one allowed for $\pi\pi$ production at DAΦNE. One see that the Z limitation results in strong limitations on X_1, X_2 that remain relatively close to Z , as well as on the rapidity of the $\gamma\gamma$ system Y. Then, one notices that the limit on rapidity given by the photon phase-space, for $W \geq 2m_\pi$, is $\mid Y \mid \leq 1.2$.

4.2 Hadronic-state decay

Looking, for example, at a two body production where $y^\star_{1,2} = \pm y^\star$ one has :

$$y_{1,2} = Y \pm y^\star$$

Assuming an angular acceptance of the central detector given by $\mid \cos\Theta_{1,2} \mid \leq \cos\Theta_0$,

so that $\mid y_{1,2} \mid \leq y_0$ with $y_0 \equiv \tanh^{-1}\cos\Theta_0$, one derives :

$$\mid y^\star \mid, \mid Y \mid \leq y_0$$

Then at KLOE, for $\cos\Theta_0 = 0.98$ one has $\mid Y \mid \leq 2.29$ and, for $Z > 0.3$ the limit on Y is in fact due to the phase space of the incident photons $\mid Y \mid \leq 1.2$, while the limits on $y^\star$ is given by $y_0 - Y$

The correlations between the differents sets of the 3 independant parameters

$(Z, Y, y^\star/\cos\Theta^\star)$ or $(X_1, X_2, y^\star/\cos\Theta^\star)$, as well as their respective integration range for $Z > 0.3$ and $\mid \cos\Theta \mid \leq 0.98$, are visualised on the following plots.

Let us note that any elementary volume on the second plot is proportional to the differential element $(dW/W)dY\,d(\cos\Theta^\star)$ with which the differential cross section $d\sigma_{\gamma\gamma}(W, \Theta^\star)/d\cos\Theta^\star$ is to be convoluted.

Now, integrating the $\gamma\gamma$ luminosity over the plateau of rapidity one obtains an angular efficiency $\epsilon_Z(\cos\Theta^\star)$ in the $\gamma\gamma$ frame which, for $Z \geq \tan\frac{\Theta_0}{2}$, depends either of the angular acceptance of the ougoing prongs or of the phase space of the incoming photons.

For $\tan\Theta^\star/2 \geq (\tan\Theta_0/2)/Z$ (i.e. $y_0 - y^\star \leq \ln(1/Z)$) one has $\epsilon_{\not Z}(y^\star) = y_0 - y^\star$

For $\tan\Theta^\star/2 \leq (\tan\Theta_0/2)/Z$ (i.e $y_0 - y^\star \geq \ln(1/Z)$) one has $\epsilon_Z(\not y^\star) = \ln(1/Z)$

The values of the angular efficiency $\epsilon_Z(\cos\Theta^\star)$ are shown in the following figure.

Let us note that, in first approximation, one has

for $Z > \tan\frac{\Theta_0}{2}$ or $\tan\frac{\Theta^\star}{2} \geq (\tan\frac{\Theta_0}{2})/Z$:

$$\frac{d\sigma_{ee\to ee XX}}{dW} \propto \frac{1}{W}\ln\frac{(1+\cos\Theta_0)(1-cos\Theta^\star)}{(1-\cos\Theta_0)(1+cos\Theta^\star)}\frac{d\sigma_{\gamma\gamma\to XX}(W,\Theta^\star)}{d\cos\Theta^\star}d\cos\Theta^\star$$

and, for $Z < \tan\frac{\Theta_0}{2}$ and $\tan\frac{\Theta^\star}{2} \leq (\tan\frac{\Theta_0}{2})/Z$:

$$\frac{d\sigma_{ee\to ee XX}}{dW} \propto \frac{1}{W}\ln\frac{2E}{W}\frac{d\sigma_{\gamma\gamma\to XX}(W,\Theta^\star)}{d\cos\Theta^\star}d\cos\Theta^\star$$

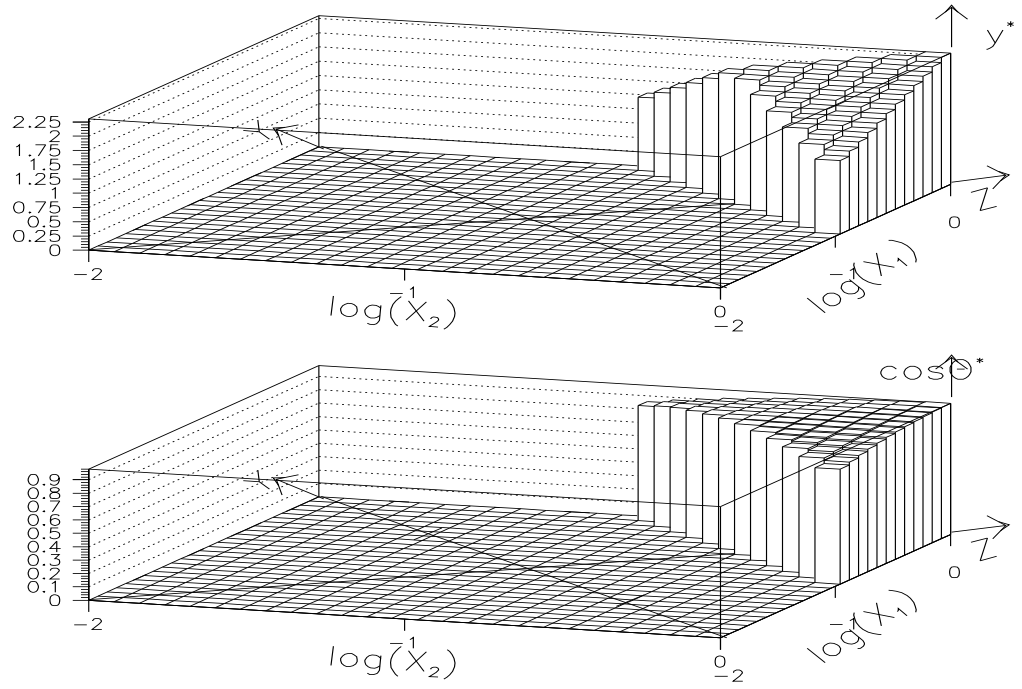

Figure 4: $(Z, Y, y^\star(\cos\Theta^\star))$ or $(X_1, X2, y^\star(\cos\Theta^\star))$ relations and integration range

4.3 $\gamma\gamma \to \pi^+\pi^-$ at DAΦNE

Up to now we have considered the two prongs as ultrarelativistic. It is obviously not the case from the $\pi\pi$ production at DAΦNE, near the threshold. This involves some differences at small W since the $\widetilde{\beta}$ and $\widetilde{\beta}^\star$ must be taken into account in $y = \tanh^{-1}\widetilde{\beta}_\pi \cos\Theta$ and $y^\star = \tanh^{-1}\widetilde{\beta}^\star_\pi \cos\Theta^\star$

The results are shown on the following plots

The differential counting rates behaviour shown in Fig.7 is the shape of the differential cross section expected for Born approximation after integration over the photon phase space and the angular acceptance. It is the product of $\epsilon_W(\cos\Theta^\star)/W$ with the differential cross section $\frac{d\sigma_{\gamma\gamma\to\pi\pi}}{d\cos\Theta^\star} = \frac{\beta^\star}{W^2}\frac{(1-\beta^{\star 2})^2+\beta^{\star 4}(1-\cos^2\Theta^\star)^2}{(1.-\beta^{\star 2}\cos^2\Theta^\star)^2}$

Kinematical constraints

Assuming the $\pi\pi$ to be produced from quasi-real photons collisions it results that there is only 4 independant parameters $E_{\gamma,1}E_{\gamma 2}, \Theta^\star$ and $\Phi^\star$ while, detecting the two pions, we measure 6 quantities $(\mid \overrightarrow{P} \mid, \Theta, \Phi)_{1,2}$.

Then, selecting events with

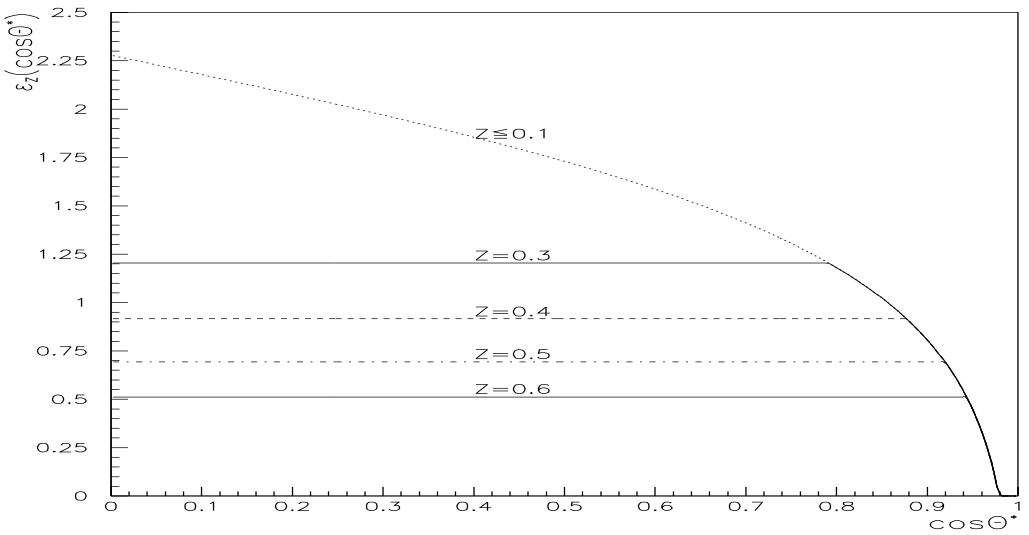

Figure 5: angular efficiency in the $\gamma\gamma$ frame for $\mid \cos\Theta \mid \leq 0.98$ in the ee frame

$$\mid \overrightarrow{P}_1 \mid \sin\Theta_1 - \mid \overrightarrow{P}_2 \mid \sin\Theta_2 = 0 \quad \text{and} \quad \Phi_1 + \Phi_2 = \pi$$

from $P_{1,2} = \mid \overrightarrow{P}_{1,2} \mid$, $E_{1,2} = \sqrt{P_{1,2}^2 + m_\pi^2}$, $\beta_{1,2} = P_{1,2}/E_{1,2}$, and $y_{1,2} = \tanh^{-1}\beta_{1,2}\cos\Theta_{1,2}$

one has:

$$y^\star \equiv \tanh^{-1}\beta^\star\cos\Theta^\star = (y_1 + y_2)/2$$
$$Y \equiv \tanh^{-1}\beta_{\gamma\gamma} = (y_1 - y_2)/2$$
$$W_{\gamma\gamma}^2 = 2(m_\pi^2 + E_1E_2 - \overrightarrow{P}_1\overrightarrow{P}_2)$$
$$E_{\gamma\gamma} = E_1 + E_2$$

from which we still derive one constaint, as for example :

$$2E_{\gamma\gamma} = W_{\gamma\gamma}\cosh Y$$

Now, in case of zero degree angle tagging system, each measurement of the energy of a tagged electron leads to an other constaint since one has:

$$E'_{1,2} = E - E_{\gamma\gamma}(1 \pm \tanh Y)$$

5 Conclusions

Let me emphasize that, for quasi-real photons, the so called DEPA (Double Equivalent Photon Approximation) consists in neglecting all terms of the order of $\mid q^2 \mid /W^2$ in the differential expression of the cross section. Monte-carlo computation does not need to neglect any angles nor to use simplified kinematic formulas. All physical parameters can be generated (including the scattering angle of the electrons Θ') and the kinematic can be also taken into account exactly.

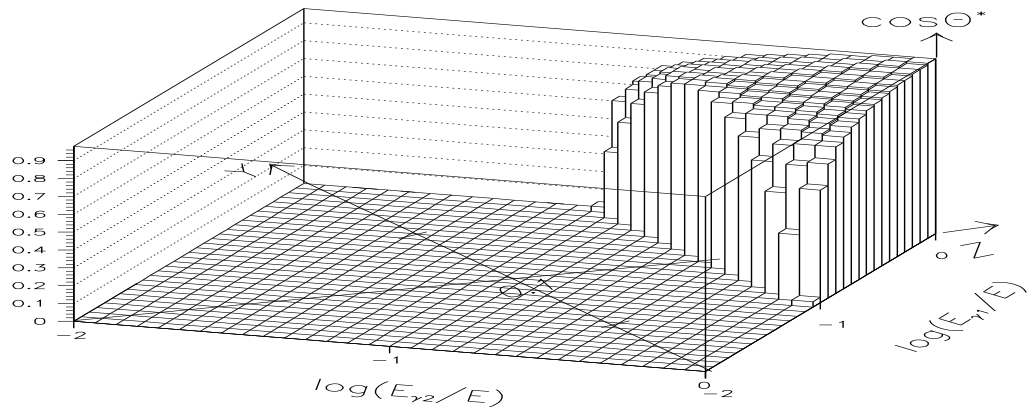

Figure 6: correlations and integration range for $\gamma\gamma \to \pi^+\pi^-$ at DAΦNE

However the simplified formulas we just discussed, allow one to describe easily or even to visualise the main features of the process, and are also helpfull in the choice of the strategy of Monte-Carlo generation and data analysis.

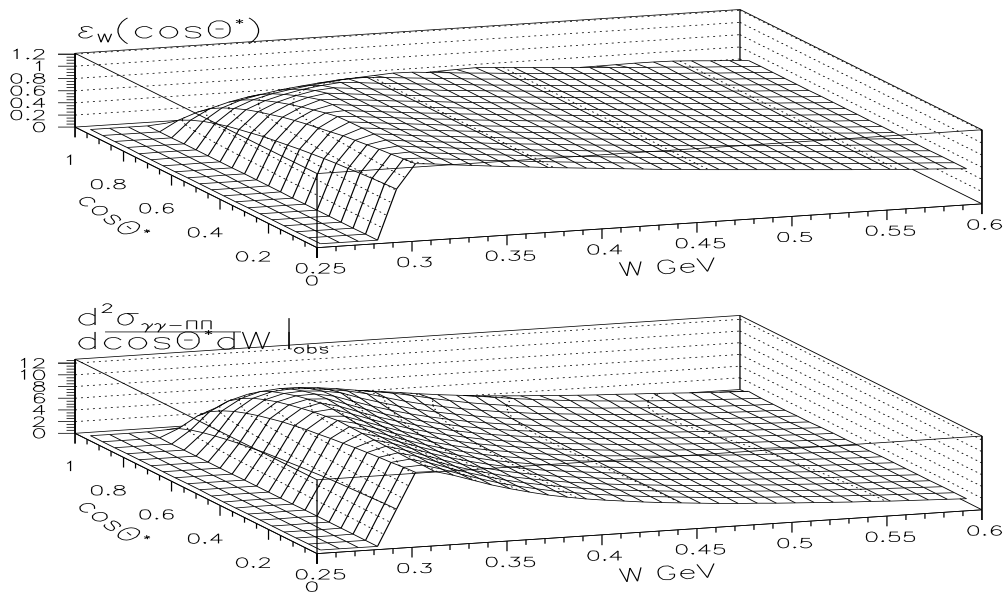

Figure 7: acceptance and counting rates behaviour for $\gamma\gamma \to \pi^+\pi^-$ at DAΦNE